Pramāna, Vol. 8, No. 2. 1977, pp. 123–132. © Printed in India.

Dispersion and spectral characteristics of crossfield instability in collisional magnetoplasma

Y C SAXENA and P I JOHN
Physical Research Laboratory, Ahmedabad 380009

MS received 3 September 1976; in revised form 8 November 1976

Abstract. Results on dispersion and spectral characteristics of crossfield instability in a collisional magnetoplasma are presented for different values of externally applied radial electric field. The dispersion relation obtained experimentally differs significantly from predictions of linear theory for strong electric fields. K-spectra for density and potential fluctuations follow power law with indices $(-3{\cdot}7 \pm 0{\cdot}5)$ and $(-5{\cdot}6 \pm 0{\cdot}6)$ respectively.

At large values of applied electric fields, the main crossfield modes appear to give rise to a number of other modes possibly through non-linear wave-wave interactions. Large amplitude $m = 2$ mode displays strong sidebands indicating particle trapping by the non-linear waves. Non-linear wave-wave and wave particle interactions, thus, appear to play an important role in the saturation of the cross field instability.

Keywords. Crossfield instability; wave-wave interactions; particle trapping.

1. Introduction

In a weakly ionised plasma, with collisional ions ($\nu_i \gtrsim \Omega_i$), magnetised electrons ($\nu_e \ll \Omega_e$) and electric field and density gradients perpendicular to the external magnetic field, there exist two types of instabilities, *viz.*, the two stream (Farley-Buneman) instability and the crossfield instability. While the former is driven by crossfield electron current due to the perpendicular electric field, the latter arises due to the density gradient parallel to the electric field. The plasma in equatorial electrojet is weakly ionized collisional plasma with above-mentioned characteristics. It is believed that the crossfield and the two-stream instabilities (Farley 1963, Buneman 1963, Whitehead 1967, Reid 1968, Rogister and D'Angelo 1970) are responsible for the density irregularities observed in equatorial electrojet region using radar backscatter (Bowles *et al* 1963, Balsley and Farley 1971) and rocket borne probes (Prakash *et al* 1969, 1971).

A laboratory experiment simulating certain essential characteristics of equatorial electrojet plasma (*viz.*, $\nu_e \ll \Omega_e$; $\nu_i \gtrsim \Omega_i$; $\boldsymbol{E} \parallel \nabla n \perp \boldsymbol{B}_0$) has been carried out with a view to understand the non-linear characteristics of these electrojet instabilities. Preliminary results on the observation of the Farley-Buneman and the crossfield instability have been reported elsewhere (John and Saxena

1975 *a*, Saxena and John 1975). In this paper we present detailed results on the dispersion and spectral characteristics of the crossfield instability and non-linear behaviour of crossfield modes for values of applied electric field far above the threshold for the crossfield instability.

2. Theory

The linear theories for the crossfield and the two stream instabilities in a weakly ionized plasma with collisional ions and magnetized electrons have been developed by a number of authors. Both the instabilities allow for a unified treatment (*e.g.*, Rogister and D'Angelo 1970, Schmidt and Gary 1973, Sato 1973). Following Rogister and D'Angelo (1970), the dispersion relation for long parallel wavelengths ($k_\parallel \ll k_\perp$) may be written as

$$\left(\frac{\nu_e}{\Omega_e\Omega_i} - i\,\frac{\chi k_y}{\Omega_i k_\perp^2}\right)\omega^2 + \left[\frac{\nu_i}{\Omega_i}\,\frac{\chi k_y}{k_\perp^2} + i\left(1 + \frac{\nu_e\nu_i}{\Omega_e\Omega_i}\right)\right]\omega$$

$$- \frac{\nu_e}{\Omega_e\Omega_i}\,c_s^2 k_\perp^2 - i\,V_d k_y = 0. \tag{1}$$

Here $\chi = \nabla n/n$, C_s is the ion-acoustic speed in plasma and V_d is the drift velocity of electrons with respect to ions. Subscripts $\parallel$ and $\perp$ refer to the directions parallel and perpendicular to the magnetic field respectively, and k_y is the wave number in the $\boldsymbol{E} \times \boldsymbol{B}$ direction. For $\chi\lambda \sim \nu_i/\Omega_e$; $\omega\nu_i > c_s^2 k_\perp^2$, ω^2 this relation may be solved to give the real part ω_r as

$$\omega_r = V_d k_y \Big/ \left(1 + \frac{\nu_e\nu_i}{\Omega_e\Omega_i}\right) \tag{2}$$

and the growth rate γ as

$$\gamma = \left[\frac{\nu_d k_y}{1 + (\nu_e\nu_i/\Omega_e\Omega_i)}\,\frac{\nu_i}{\Omega_i}\,\frac{\chi k_y}{k_\perp^2} + \frac{\nu_e}{\Omega_e\Omega_i}\,(\omega^2 - c_s^2 k_\perp^2)\right] \Big/ \left(1 + \frac{\nu_e\nu_i}{\Omega_e\Omega_i}\right). \tag{3}$$

However, for $\chi\lambda \sim \Omega_i/\nu_i$, $\omega_r \sim \Gamma$ the dispersion relation gives the real part as

$$\omega_r \simeq V_d k_y \Big/ \left[1 + \left(\frac{\nu_i}{\Omega_i}\,\frac{\chi k_y}{k_\perp^2}\right)^2\right] \tag{4}$$

and the growth rate as

$$\Gamma \simeq \gamma \Big/ \left[1 + \left(\frac{\nu_i}{\Omega_i}\,\frac{\chi k_y}{k_\perp^2}\right)^2\right]. \tag{5}$$

In the later case, for low frequency regime, the growth rate is of the order of the real part of the frequency and waves are dispersive in nature (Rogister 1972). Quasi-linear theories of the electrojet instabilities including local velocity retardation have been given by Sato (1971, 1972) and Rogister (1972). Sato (1971) predicts the development of strong turbulence in the plasma in which a number of modes are strongly excited and interact with each other. Rogister (1972) has presented a non-linear theory in which energy is transferred by mode-coupling from large to small wavelengths where it is absorbed by linear damping. Sato

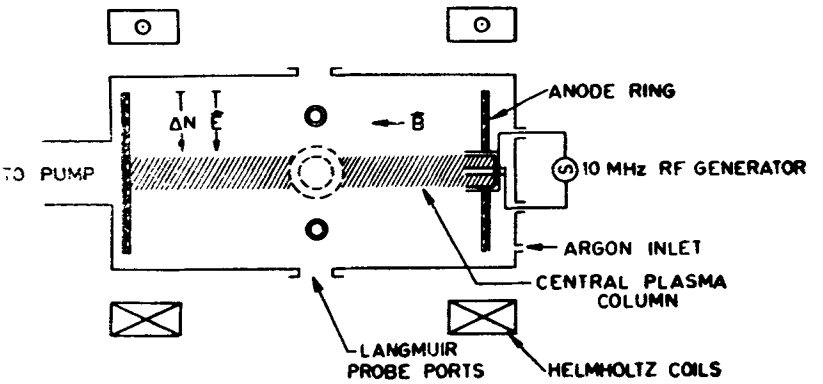

Figure 1. A schematic diagram of the experimental system for study of equatorial electrojet instabilities in laboratory plasma.

(1976) has given a complete quasi-linear theory of the electrojet instabilities which includes the local density deformation in addition to the conventional electron drift retardation. He concludes that the dominant quasi-linear stabilization process for the crossfield instability is the flattening of density profile for normal electrojet conditions. Actually, however, mode coupling may play an important role (Sato 1976).

3. Experimental set-up

A schematic of the experimental system is given in figure 1. The system, described in detail by John and Saxena (1975 *b*) consists of a cylindrical non-magnetic stainless steel chamber of 30 cm diameter and 60 cm length. Axially uniform magnetic field is produced in the experimental region by means of a pair of Helmholtz coils. The field strength can be continuously varied up to $\sim$ 500 Gauss by means of an adjustable constant current source. After evacuation to a pressure of $\sim 10^{-5}$ torr the chamber is filled with argon gas at a pressure of 1 mtorr. Plasma is produced by the ionization of the gas by means of a RF discharge between the two coaxial cylindrical conductors (0·5 cm and 5 cm in dia; 5 cm in length) at one end of the chamber. The plasma diffusing out from the axial uniform dense region fills the chamber. Radial density gradients, directed inwards, exist in the plasma. Radial electric field is imposed on the plasma by applying a graded potential to a set of annular ring anodes which serve as an axial boundary for the plasma. By giving a variable differential d.c. bias, the radial electric field can be changed.

Radially movable Langmuir probes placed at various azimuthal and axial separations together with current-to-voltage converters and voltage followers are used for diagnostics. Fluctuations in potential and ion densities are picked up by floating high impedance probes and negatively biased low impedance probes respectively.

Phase differences between azimuthally and axially separated probes are used to determine the azimuthal mode numbers and measure the phase velocities in azimuthal and axial directions respectively. An on-line spectrum analyser is used to get spectra of the instabilities.

4. Results and discussions

The potential and density profiles for the plasma in the present set-up are shown in figure 2. Beyond the production region (for radii $> 2{\cdot}5$ cm) there exist inward electric field and density gradients. Low frequency waves travelling in $\boldsymbol{E} \times \boldsymbol{B}$ direction are observed beyond a certain threshold value of the magnetic field ($B_0 \gtrsim 100$ Gauss). The electron temperature in the plasma is $\sim 2{\cdot}5$ eV. Instability measurements are made at a radius of 7 cm in a magnetic field of 190 Gauss. By varying the potential across the end electrode, the electric field at 7 cm is varied from $1{\cdot}29$ v/cm to $2{\cdot}2$ v/cm. The scale sizes for the density gradient varies between 3 cm to 4 cm.

Signals picked up simultaneously with two probes placed at the same radius and azimuth but separated axially by 30 cm do not show any phase shift which indicates that the observed instability has very long parallel wavelength (wavelengths much larger than machine length). The possibility of excitation of parallel wavelengths greater than twice the machine length due to the presence of ion-sheaths at the end of plasma column has been pointed out by Chen (1965) for the case of drift instabilities, and confirmed for the case of crossfield instability by Saxena and John (1975).

Azimuthally separated probes indicate that the waves are travelling azimuthally in $\boldsymbol{E} \times \boldsymbol{B}$ direction. From mode numbers measured using azimuthally separated probes, and the frequencies from the spectrum analyser, the dispersion relation for the instability has been obtained. Figure 3 shows (ω, k) plot for five different values of electric fields. The curves numbered 1, 2, 3, 4 and 5 correspond to electric field values of $1{\cdot}29$ v/cm, $1{\cdot}37$ v/cm, $1{\cdot}42$ v/cm, $1{\cdot}44$ v/cm and $1{\cdot}48$ v/cm respectively. The observed waves are low frequency waves with $\omega < C_s K_\perp$ and

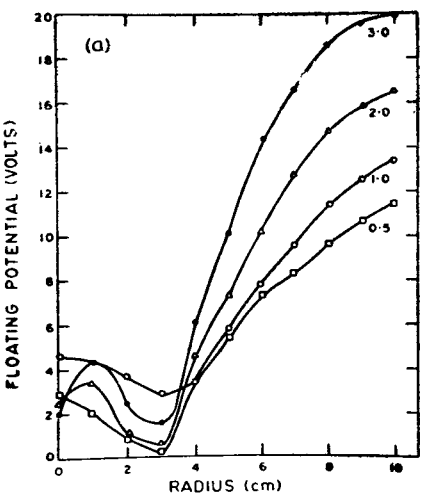

Figure 2 *a*. Radial potential profiles in plasma for different magnetic fields. (1 amp. current ≡ 95 Gauss magnetic field strength).

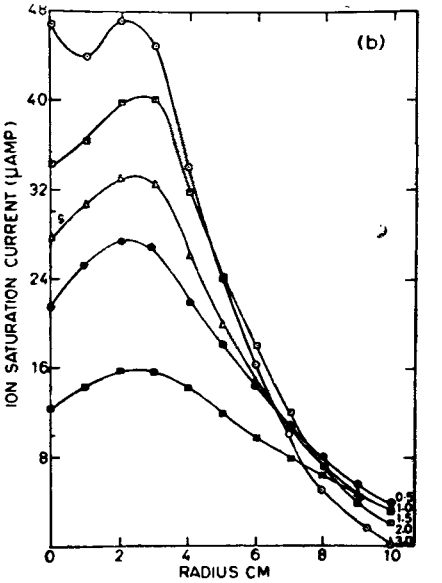

Figure 2 *b*. Radial density profiles in plasma for different magnetic field (1 μA ion saturation current ≡ 3×10^8 particles/cm^3).

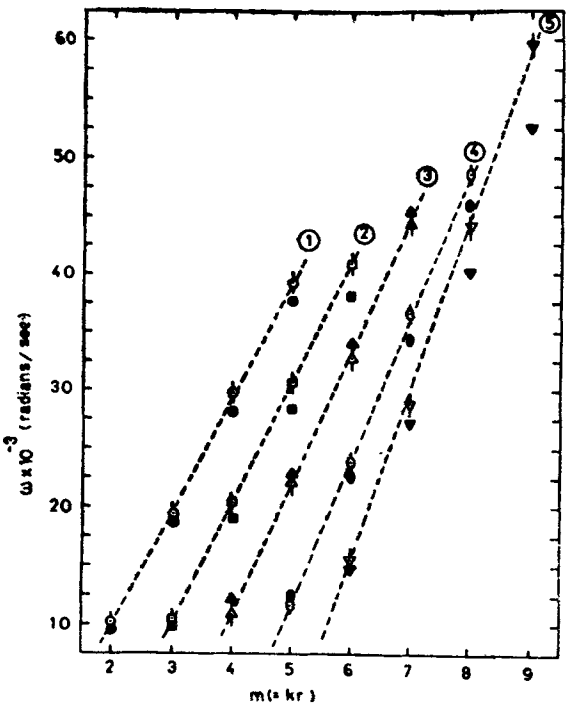

Figure 3. Dispersion relation for the crossfield instability. Horizontal scale gives azimuthal mode number m and vertical scale the frequency ω. Shaded points are calculated values of ω from linear theory [eq. (1)]. Horizontal scales are shifted to right by 1 div. for succeeding curves. The numbers 1, 2, 3, 4 and 5 correspond to electric field values of 1·29 v/cm, 1·37 v/cm, 1·42 v/cm, 1·44 v/cm and 1·48 v/cm.

are thus not generated by two-stream (Farley-Buneman) instability. In present case $\chi \simeq 0{\cdot}25\ \text{cm}^{-1}$, $\lambda \gtrsim 10$ cm and $\Omega_i/\nu_i \simeq 0{\cdot}1$. Thus the instabilities observed here belong to a domain where $\chi\lambda \gtrsim \Omega_i/\nu_i$. Calculations based on linear theory suggest that the observed modes are fast growing crossfield modes of the type predicted by Rogister (1972) for $\chi\lambda \gtrsim \Omega_i/\nu_i$. The waves are dispersive as expected on the basis of the linear theory. Also shown simultaneously in figure 3 are the predictions of the linear theory based on eq. (1). One notes a relatively good agreement between the observations and theoretical predictions for electric field values of 1·29 v/cm and 1·42 v/cm. There is a slight discrepancy between the observation and the theory at 1·37 v/cm. However, at large electric fields one sees a significant deviation from theoretical predictions for larger $k_\perp$ values. A frequency-shift from the linear theory is clearly indicated and such a shift might arise out of certain non-linearities. In the case of two-stream instability a frequency shift due to non-linear effects has been predicted by Weinstock and Rognlien (1975). Non-linear theory of Rogister (1972) indicates a non-linear frequency shift in dispersionless regime [second term in eq. 15 of the paper of Rogister

(1972) represents non-linear frequency shift]. It is desirable to make a quantitative comparison between the observed dispersion relation and predictions of the non-linear theories. However, non-linear theories such as those of Rogister (1972) and Sato (1976), do not give any explicit expression for the non-linear dispersion relation and thus such a comparison is not possible without doing extensive numerical calculations for solving the non-linear equations given by these theories. The comparison at this stage then has to be necessarily qualitative.

We also note the conspicuous absence of $m = 1$ mode at all electric fields The lowest observed mode is $m = 2$. Attempts have been made to improve the low frequency response of the probes and yet $m = 1$ mode is not observed. It may be mentioned that in our earlier observations (Saxena and John 1975) also, whe e spectrum analysis was done digitally, the lowest mode observed was $m = 2$. The reason for absence of $m = 1$ mode is not clear.

The k-spectra for the density and potential fluctuations are shown in figure 4. The spectra follow power law and have indices of $(-3{\cdot}7 \pm 0{\cdot}5)$ and $(-5{\cdot}6 \pm 0{\cdot}6)$ respectively. The index of $(-3{\cdot}7 \pm 0{\cdot}5)$ for density fluctuations is in good agreement with the spectral index of $(-3{\cdot}0 \pm 1{\cdot}0)$ obtained in *in-situ* rocket measurements by Prakash *et al* (1969). The index also agrees well with the spectral index of -3 given by Ott and Farley (1974) on dimensional ground

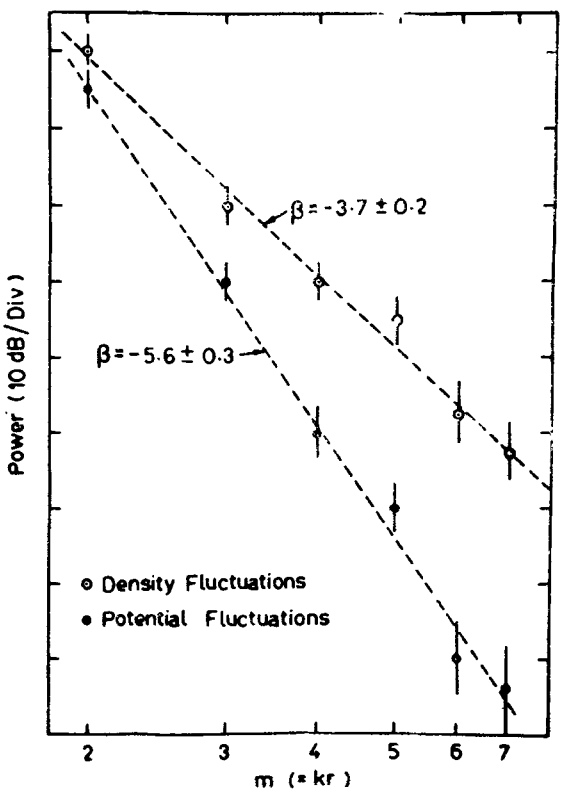

Figure 4. K-spectra for the density (⊙) and potential fluctuations (●). The lines drawn through the experimental points are obtained by least square fit to a power law.

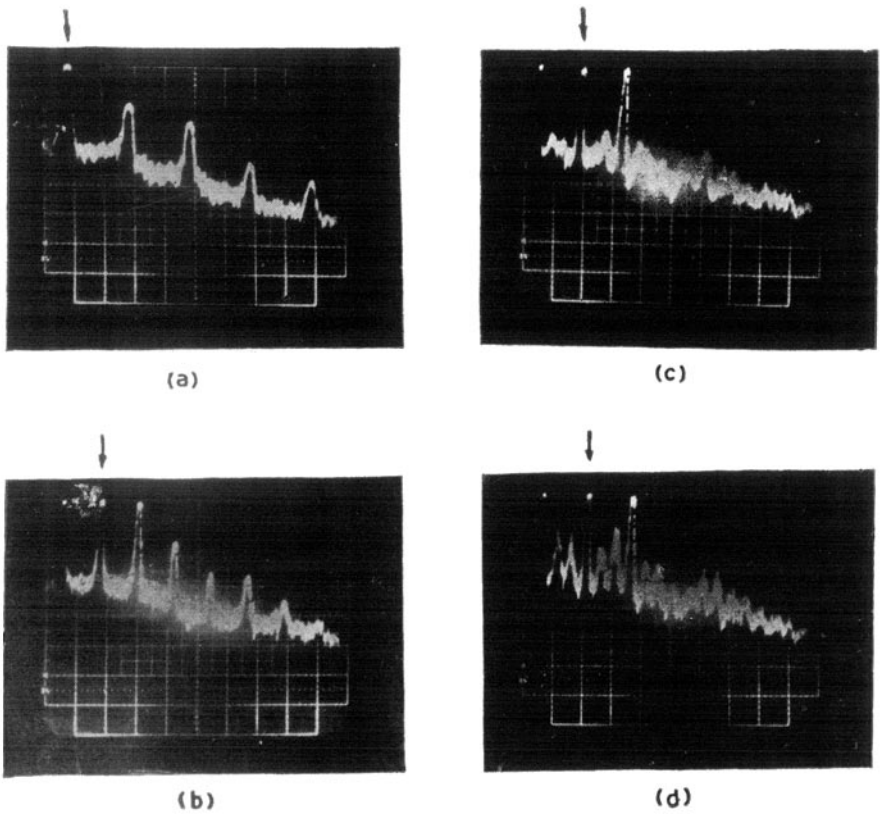

Figure 5. Power spectra of density fluctuations for different electric fields: (*a*) 1·44 v/cm, (*b*) 1·48 v/cm, (*c*) 1·63 v/cm and (*d*) 2·28 v/cm. The horizontal scale in (*a*) is 1 KHz/div. while for rest of the spectra the scale is 2 KHz/div. Arrows indicate zero frequency on each spectra.

and the index of $-3{\cdot}5$ obtained by McDonald *et al* (1975) from a numerical simulation. The power spectrum for potential fluctuations is steeper than that for density fluctuations, the difference between the spectral indices being ~ 2.

Sato and Ogawa (1976) have numerically studied in detail two-dimensional structure of the crossfield instability. Calculations give the power spectral shape of k^{-3} for density irregularities in the $(\boldsymbol{E} \times \boldsymbol{B})$ direction. Power spectral shape of potential irregularities is found to be of K^{-6} type. The present observations are in reasonable agreement with these calculations.

In figure 5 we present a series of observed spectra of density fluctuations for different electric field values. One notes the appearance of a turbulent spectrum for fields beyond 1·48 v/cm accompanied by reduction in the amplitude of some higher normal modes and appearance of a number of modes other than the normal crossfield modes. It thus appears that as the crossfield modes grow more and more non-linear, they interact with each other and give rise to number of other modes through non-linear wave-wave interactions. Sato (1971, 1976) inferred from the non-linear treatment of the crossfield instability that a strong turbulence is realised and a number of modes are strongly excited and interact with each other. Non-linear theory of Register (1972) also predicts energy transfer by mode coupling from large to small wavelengths where it is absorbed by linear damping. The observations presented here appear to support such points of view. It may be mentioned here that in our earlier observations (Saxena and John 1975) at an electric field of 2·0 v/cm, we observed $m = 1$ and $m = 0$ modes besides the normal crossfield modes and were able to identify these modes to the ones generated through wave-wave interactions of the normal crossfield modes by verifying the wave number and frequency matching conditions.

We also note (figures 5 *c* and 5 *d*) the appearance of side bands of $m = 2$ mode indicating particle trapping by the non-linear waves. At an electric field of 1·63 v/cm (figure 5 *c*) the $m = 2$ mode with $\omega_2 = 17{\cdot}1 \times 10^3$ radians/sec displays lower sideband at $\omega = 10{\cdot}3 \times 10^3$ radians/sec and the upper sideband at $24{\cdot}0 \times 10^3$ radians/sec, the difference in frequency from the main mode for the sidebands being approximately $\triangle\omega \simeq \pm 6{\cdot}9 \times 10^3$ radians/sec. Similarly at an electric field of 2·28 v/cm (figure 5 *d*) the $m = 2$ mode at $\omega_2 = 18{\cdot}5 \times 10^3$ radians/sec displays two sidebands at $\triangle\omega = \pm 6{\cdot}0 \times 10^3$ radians/sec and $\triangle\omega \simeq \pm 12{\cdot}00 \times 10^3$ radians/sec. Non-linear theories of crossfield instability do not take the particle trapping into account. However, the present observations indicate that wave-particle interactions leading to particle trapping might play important role in saturation of the crossfield instability.

5. Conclusions

(i) Dispersion characteristics of the crossfield instability obtained experimentally for different values of applied electric field indicate a good agreement with linear theory for small values of electric field but divert significantly from the theoretical predictions for large values of electric fields. A non-linear frequency shift from linear theory predictions is indicated.

(ii) The spectral indices for the potential and density fluctuations have values of $(-5{\cdot}6 \pm 0{\cdot}6)$ and $(-3{\cdot}7 \pm 0{\cdot}5)$ respectively.

(iii) Non-linear wave-wave and wave-particle interactions appear to play important role in the saturation mechanism of the crossfield instability as demonstrated by appearance of number of modes and side-bands of normal modes at large electric fields.

References

Balsley B B and Farley D T 1971 *J. Geophys. Res.* **76** 8341
Bowles K L, Balsley B B and Cohen R 1963 *J. Geophys. Res.* **68** 2488
Buneman O 1963 *Phys. Rev. Lett.* **10** 285
Chen F F 1965 *Phys. Fluids* **8** 752
Farley D T 1963 *Phys. Rev. Lett.* **10** 4747
John P I and Saxena Y C 1975 *a Geophys. Res. Lett.* **2** 251
John P I and Saxena Y C 1975 *b Indian J. Radio Space Phys.* **4** 267
McDonald B E, Coffey T P, Ossakow S and Sudan R N 1975 *Radio Sci.* **10** 247
Ott E and Farley D T 1974 *J. Geophys. Res.* **79** 2469
Prakash S, Gupta S P and Subbaraya B H 1969 *Radio Sci.* **4** 791
Prakash S, Gupta S P and Subbaraya B H 1971 *Nature Phys. Sci.* **230** 170
Reid G C 1968 *J. Geophys. Res.* **73** 1627
Rogister A 1972 *J. Geophys. Res.* **77** 2975
Rogister A and D'Angelo N 1970 *J. Geophys. Res.* **75** 3879
Sato T 1971 *Phys. Fluids* **14** 2426
Sato T 1972 *Phys. Rev. Lett.* **28** 732
Sato T 1973 *J. Geophys. Res.* **78** 2232
Sato T 1976 *J. Geophys. Res.* **81** 5139
Sato T and Ogawa T 1976 *J. Geophys. Res.* **81** 3248
Saxena Y C and John P I 1975 *Geophys. Res. Lett.* **2** 492
Schmidt K J and Gary S Peter 1973 *J. Geophys. Res.* **78** 8261
Weinstock J and Rognlien T D 1975 *Radio Sci.* **10** 231
Whitehead J D 1967 *J. Atmos. Terr. Phys.* **29** 1285